Proceedings of Computational Engineering Conference JSCES
Vol. 28, 2023 May

Numerical Simulation of the Interactions between an Off-road Pneumatic Tire and Gravel Terrain Using a Multi-sphere DE-FE Method

Xiaobing Guo[1)], Zumei Zheng[2)], Naoto Mitsume[3)], Mengyan Zang[4)] and Shunhua Chen[5)]

1) Ph.D (Institute of Systems and Information Engineering, University of Tsukuba 1-1-1, Tennodai, Tsukuba, Ibaraki, 305-8573, Japan, E-mail: guo.xiaobing.gn@u.tsukuba.ac.jp)

2) Ph.D (School of Mechanical Engineering, Qilu University of Technology, Jinan, 250353, China, E-mail: zhengzumei10@qlu.edu.cn)

3) Assistant Professor (Institute of Systems and Information Engineering, University of Tsukuba 1-1-1, Tennodai, Tsukuba, Ibaraki, 305-8573, Japan, E-mail: mitsume@kz.tsukuba.ac.jp)

4) Professor (School of Mechanical & Automotive Engineering, South China University of Technology, Guangzhou, 510641, China, E-mail: myzang@scut.edu.cn)

5) Associate Professor (School of Marine Engineering and Technology, Sun Yat-sen University, Zhuhai, 519082, China, E-mail: chenshunhuascut@gmail.com)

In this work, a combined multi-sphere discrete element and finite element (DE-FE) method is developed to simulate the interactions between an off-road pneumatic tire and gravel terrain in a natural way. Firstly, several kinds of multi-sphere gravel particle models (GPMs) are established, and the multi-sphere DE-FE model is constructed on the basis of the soil-bin experiment. Then the tractive performance of an off-road pneumatic tire on gravel terrain is simulated. The results show that the simulation results obtained by the multi-sphere DE-FE method are consistent with the experimental data, and our developed method can reproduce the tractive behavior of off-road tires on gravel terrain well.

Key Words : *Multi-sphere DE-FE method, Tractive performance, Soil-bin experiment*

1. INTRODUCTION

The interactions between off-road tire and granular terrain have a great influence on the tractive performance of tire, and are attracting more and more attention from scholars in vehicle engineering. In recent years, many numerical techniques have proposed to investigate the tire-terrain interactions, such as discrete element method (DEM) [1], finite element method (FEM) [2] and combined discrete element-finite element (DE-FE) method [3–5]. In the combined DE-FE method, the FEM was used to describe the large deformation of the off-road tire, while the DEM was employed to capture the discontinuous characteristics of granular terrain.

Even though the combined DE-FE method can basically simulate the traveling behaviors of a tire on granular terrain, the granular particles were usually described by using circular DEs (in the two-dimension simulation) or spherical DEs (in three-dimensions), which may affect the computational accuracy of simulation results. In view of this, some researchers proposed two main approaches to model non-spherical granular particles: one is to add an artificial rolling resistance moment or a shape parameter in spherical DEs to deal with the interlocking mechanism between irregular granular particles; The other one is to establish a more accurate particle model, such as ellipsoid model, polyhedron model and multi-sphere model. In this work, a multi-sphere DE-FE method is developed to handle the interactions between an off-road tire with smooth tread and gravel terrain by using multi-sphere model.

2. MODELING OF GRAVEL PARTICLES

The multi-sphere model, proposed by Favier et al. [6], is an approximation method to simulate the non-spherical shapes of real granular particles, where one multi-sphere particle can be constructed using a set of elemental spheres. In our soil-bin experiment, all gravel particles are filtered by the sieving test to keep the particle sizes within a specified range, i,e., the radii of gravel particles are distributed from 5 to 7 mm randomly, as illustrated in Fig. 1. Herein, three simple kinds of multi-sphere gravel particle models (GPMs) are established, i.e., cylindrical GPM, conical GPM and cubical GPM, as shown in Fig. 2.

Fig. 1 Gravel particles

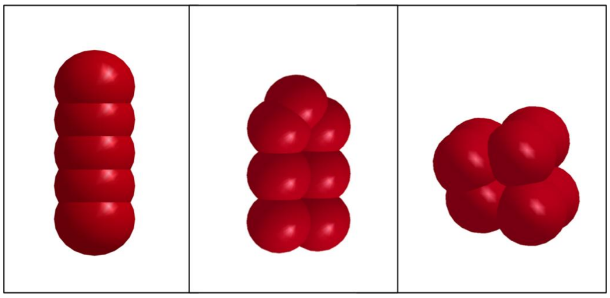

Fig. 2 Modeling diagram of multi-sphere GPMs

3. COMBINED METHOD OF MULTI-SPHERE DES AND FES

For the contact calculations of multi-sphere DEs and FEs, the inside-outside algorithm [7] is carried out to determine the contact types and the Hertz-Mindlin contact Model [8] is carried out applied in the calculations of contact forces.

(1) Contact types

Fig. 3 shows three potential contact regions between an elemental sphere and a FE segment, i.e., point-to-facet (PTF), point-to-edge (PTE) and point-to-node (PTN).

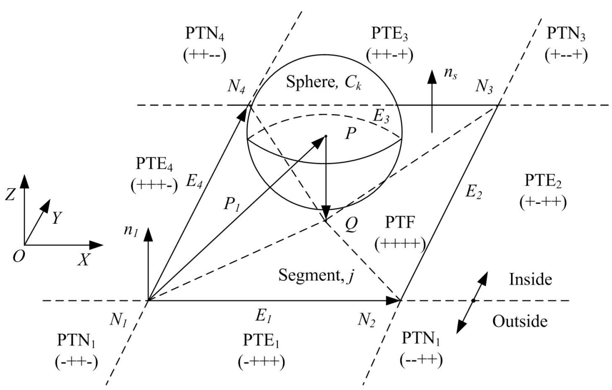

Fig. 3 Three potential contact regions: PTF, PTE and PTN

Firstly, the normal vector of FE segment at each node can be defined by the cross product of two connective edge vectors:

$$\boldsymbol{n}_i = \boldsymbol{E}_i \times (-\boldsymbol{E}_i) \ \ (i = 1, 2, 3, 4) \tag{1}$$

where $\boldsymbol{E_i}$ is the edge vector, and $\boldsymbol{E}_0$ is equivalent to $\boldsymbol{E}_4$.

Hence, the normal vector of FE segment is determined as:

$$\boldsymbol{n}_s = \sum_{i=1}^{4} \boldsymbol{n}_i \Big/ \left| \sum_{i=1}^{4} \boldsymbol{n}_i \right| \tag{2}$$

Secondly, the judgement value can be calculated by:

$$\varphi_i = (\boldsymbol{E}_i \times \boldsymbol{P}_i) \cdot \boldsymbol{n}_s \ \ (i = 1, 2, 3, 4) \tag{3}$$

where $\boldsymbol{P}_i$ is the direction vector form point N_i to point P.

Finally, the contact types can be determined by the judgement values:

a) PTF contact type: When $\varphi_i > 0 \ \ (i = 1, 2, 3, 4)$, the elemental sphere may be in contact with the facet of FE segment, and the coordinate of projection point Q can be calculated by the following formula:

$$\boldsymbol{X}_Q = \sum_{i=1}^{4} \phi_i \boldsymbol{X}_{N_i} \ \ (i = 1, 2, 3, 4) \tag{4}$$

where $\boldsymbol{X}_{N_i}$ is node coordinates; ϕ_i is the shape functions, and $\phi_1 = \varphi_2\varphi_3/\varphi$, $\phi_2 = \varphi_3\varphi_4/\varphi$, $\phi_3 = \varphi_4\varphi_1/\varphi$, $\phi_4 = \varphi_1\varphi_2/\varphi$, $\phi = (\varphi_1+\varphi_3)/(\varphi_2+\varphi_4)$.

In this case, the penetration between elemental sphere and FE segment is defined by:

$$h_{es} = (\boldsymbol{X}_P - \boldsymbol{X}_Q) \cdot \boldsymbol{n}_s - r \tag{5}$$

where X_P is the center coordinate of elemental sphere, and r is the radius. If $h_{es} < 0$, the elemental sphere contacts the facet of FE segment. If $h_{es} \geq 0$, the contact is not occur.

b) PTE contact type: When $\varphi_1 < 0$ and $\varphi_i < 0$ $(i = 2, 3, 4)$, the elemental sphere may contact edge E_1 (so do as other edges). The unit vector $\boldsymbol{e}_{E_1}$ of the edge is given by:

$$\boldsymbol{e}_{E_1} = (\boldsymbol{X}_{N_2} - \boldsymbol{X}_{N_1}) / |\boldsymbol{X}_{N_2} - \boldsymbol{X}_{N_1}| \tag{6}$$

The projection point on edge is defined by:

$$\boldsymbol{X}_Q = \boldsymbol{X}_{N_1} + (\boldsymbol{X}_{N_2} - \boldsymbol{X}_{N_1}) \cdot t_{N_1} \tag{7}$$

In which,

$$t_{N_1} = \left((\boldsymbol{X}_P - \boldsymbol{X}_{N_1}) \cdot \boldsymbol{e}_{E_1} \right) / |\boldsymbol{X}_P - \boldsymbol{X}_{N_1}| \tag{8}$$

The penetration can be calculated by:

$$h_{es} = |\boldsymbol{X}_P - \boldsymbol{X}_Q| - r \tag{9}$$

If $h_{es} < 0$, the contact between elemental sphere and the edge of FE segment is occur. If $h_{es} \geq 0$, no contact.

c) PTN contact type: When $\varphi_1 < 0$, $\varphi_2 > 0$, $\varphi_3 > 0$ and $\varphi_4 < 0$, the elemental sphere contacts point N_1 (so do as other nodes) and the penetration is:

$$h_{es} = \left|\boldsymbol{X}_P - \boldsymbol{X}_{N_1}\right| - r \tag{10}$$

If $h_{es} < 0$, the elemental sphere and the FE segment will be in contact. Otherwise, the contact does not occur.

(2) Contact forces

As depicted in Fig. 4, the contact forces between an elemental sphere in multi-sphere particle i and a FE segment j can be calculated by:

$$\boldsymbol{F}^c_{n,i_{C_k}j} = \boldsymbol{F}_{n,i_{C_k}j} + \boldsymbol{F}_{t,i_{C_k}j} \tag{11}$$

where $\boldsymbol{F}_{n,i_{C_k}j}$ and $\boldsymbol{F}_{t,i_{C_k}j}$ are, respectively, the normal and tangential contact forces, and can be obtained by:

$$\boldsymbol{F}_{n,i_{C_k}j} = k_{n,i_{C_k}j}\boldsymbol{h}_{i_{C_k}} + \gamma_{n,i_{C_k}j}\boldsymbol{v}_{n,i_{C_k}j} \tag{12}$$

When $\left|\boldsymbol{F}_{t,i_{C_k}j}\right| < \mu\left|\boldsymbol{F}_{n,i_{C_k}j}\right|$, the tangential contact forces are:

$$\boldsymbol{F}_{t,i_{C_k}j} = k_{t,i_{C_k}j}\boldsymbol{\sigma}_{i_{C_k}j} + \gamma_{t,i_{C_k}j}\boldsymbol{v}_{t,i_{C_k}j} \tag{13}$$

Otherwise, the tangential contact forces are given by:

$$\boldsymbol{F}_{t,i_{C_k}j} = \mu\boldsymbol{F}_{n,i_{C_k}j} \tag{14}$$

where $\boldsymbol{h}_{i_{C_k}}$ represents the penetration calculated by the above section. $\boldsymbol{v}_{n,i_{C_k}j}$ and $\boldsymbol{v}_{t,i_{C_k}j}$ are the normal and tangential relative velocities on the contact point, respectively; $\boldsymbol{\sigma}_{i_{C_k}j}$ is the tangential relative displacement; $k_{n,i_{C_k}j}$ and $k_{t,i_{C_k}j}$ mean the normal and tangential stiffness, respectively, which can be defined as:

$$\begin{aligned} &k_{n,i_{C_k}j} \\ &= \frac{4}{3}\left(E_{i_{C_k}}E_j\Big/\left(E_{i_{C_k}}\left(1-\upsilon_j^2\right) + E_j\left(1-\upsilon_{i_{C_k}}^2\right)\right)\right)R_{i_{C_k}}^{1/2}h_{es}^{1/2} \\ &k_{k,i_{C_k}j} \\ &= \frac{16}{3}\left(G_{i_{C_k}}G_j\Big/\left(G_{i_{C_k}}\left(1-\upsilon_j\right) + G_j\left(1-\upsilon_{i_{C_k}}\right)\right)\right)R_{i_{C_k}}^{1/2}h_{es}^{1/2} \end{aligned} \tag{15}$$

where $E_{i_{C_k}}$ and E_j denote the Young's moduli of the multi-sphere particle and the finite element, respectively; $\upsilon_{i_{C_k}}$ and υ_j are the Poisson's ratios, respectively; $G_{i_{C_k}}$ and G_j are the equivalent elastic shear moduli, that is:

$$\begin{aligned} G_{i_{C_k}} &= E_{i_{C_k}}\Big/\left(2\left(1+\upsilon_{i_{C_k}}\right)\right) \\ G_j &= E_j\Big/\left(2\left(1+\upsilon_j\right)\right) \end{aligned} \tag{16}$$

$\gamma_{n,i_{C_k}j}$ and $\gamma_{t,i_{C_k}j}$ denote the normal and tangential damping coefficients, and they can be calculated as:

$$\begin{aligned} \gamma_{n,i_{C_k}j} &= -\zeta_{n,i_{C_k}j}m_{i_{C_k}}m_j\Big/\left(m_{i_{C_k}}+m_j\right) \\ \gamma_{t,i_{C_k}j} &= -\zeta_{t,i_{C_k}j}m_{i_{C_k}}m_j\Big/\left(m_{i_{C_k}}+m_j\right) \end{aligned} \tag{17}$$

where $m_{i_{C_k}}$, m_j, $\zeta_{n,i_{C_k}j}$ and $\zeta_{t,i_{C_k}j}$ are the mass and the damping factors in the normal and tangential directions, respectively.

Additionally, $R_{i_{C_k}j}$ is the equivalent radius of elemental sphere and FE, $R_{i_{C_k}j} = R_{i_{C_k}}R_j\Big/\left(R_{i_{C_k}}+R_j\right)$, which is equal to the radius of element sphere here.

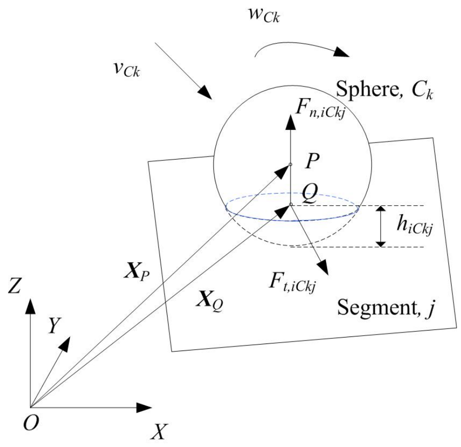

Fig. 4 Contact forces between elemental sphere and FE segment

4. EXPERIMENT AND SIMULATION MODEL

In order to analyze the tractive performance of an off-road tire on gravel terrain, an indoor soil-bin experiment device was developed in this section, which includes (1) single wheel test device, (2) soil mixing and compacting device and (3) soil-bin and control system, as depicted in Fig. 5. Among them, the nominal size of off-road tire is 37×12.5R16.5AR117 with a radius of 445 mm and a width of 310 mm.

To correspond with the soil-bin experiment, a combined multi-sphere DE-FE model is established, as shown in Fig. 6, where the gravel terrain is constructed by using multi-sphere GPMs, and the FE method is used to model the off-road tire. In the FE tire modeling, the rubber parts of the tire, including tread, sidewall, belt and carcass rubber, are modeled using the Mooney-Rivlin constitutive model, whereas the carcass and belt reinforcements of tire are described by the orthotropic elastic model. Besides, the rim is set to be rigid.

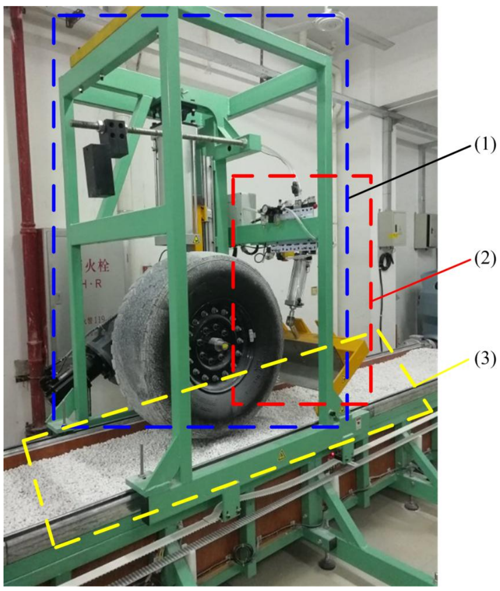

Fig. 5 Indoor soil-bin experiment device

Furthermore, many scholars mostly calibrate the contact and model parameters using the triaxial compression test or biaxial compression test. In this work, an indoor triaxial test is also performed to calibrate the simulation parameters of the multi-sphere DE-FE model, and it can be found in Ref. [9].

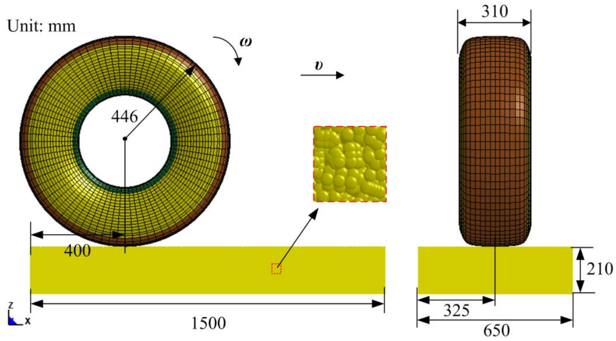

Fig. 6 Combined multi-sphere DE-FE model

The simulation process of an off-road tire on gravel terrain is composed of the following steps:

a) Inflation: The pressure of tire is increased gradually from 0 to 0.35 MPa within 10 ms, and then is kept to be constant.

b) Force loading: The vertical load acting on the rim is 10,163 N within 10-12 ms, and remains stable after 12 ms.

c) Velocity loading: the velocities will be loaded on the rim of tire directly from 0 to the prescribed value (12 to 15 ms).

d) Data analysis: the evaluation indexes of the tractive performances, including vertical reaction force, tractive force and rim sinkage, will be collected and analyzed.

5. RESULTS AND DISCUSSIONS

Fig. 7 depicts the simulation and experimental results of the traveling tracks of an off-road trie with smooth tread on multi-sphere gravel terrain under the slip rate of 20%, and the displacements of gravel particles in the Z-direction under different moments. It can be observed that the displacements of gravel particles are positive on both side berms of the tire tracks due to the extrusion of tire, whereas the displacements are negative under the off-road tire owing to the tire vertical force. As can be seen from the figure, the simulation results are in agreement with the soil-bin experimental phenomenon.

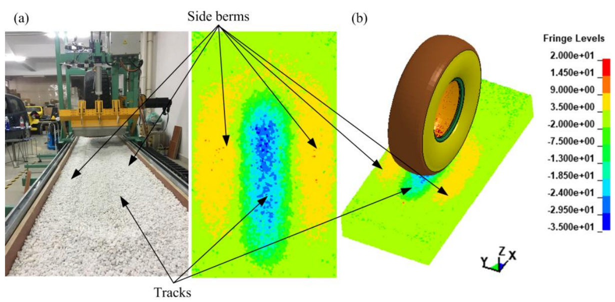

Fig. 7 Traveling tracks: (a) experiment; (b) simulation

To analyze the tractive performance of off-road tire, the vertical reaction forces of the tire on gravel terrain are illustrated in Fig. 8. In the inflation stage (i.e., 0-10 ms), the vertical reaction forces are 0 N, because the tire is not contacts with gravel terrain. With the force loading, the forces will increase rapidly within a short time. Finally, they will be gradually stabilize after a period of fluctuation because of the balance of the forces in the vertical direction.

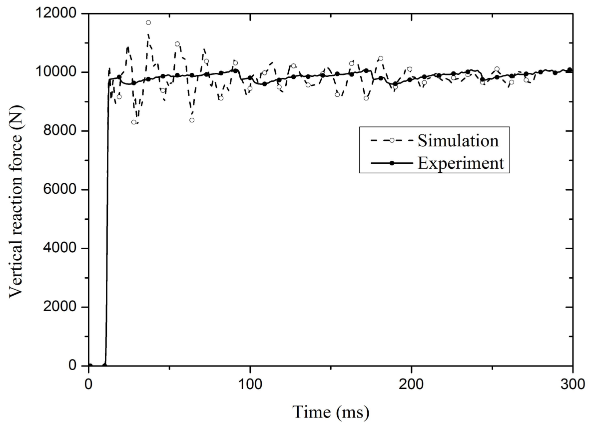

Fig. 8 Simulation and experimental results in terms of vertical reaction force history

Fig. 9 shows the simulation and experimental results of the treactive force histories. It can be found that the tractive forces dramatically increase at first to overcome the running resistance, after that the forces decrease. Finally, the tractive forces will tends to be stable, and the simulation value of the tractive force is close to that of the soil-bin experiment.

Moreover, the simulation and experimental results of the rim sinkages are shown in Fig. 10. During the force loading, the rim sinkages of off-road tire increase rapidly with the rise of the vertical forces. Since the gravel terrain is compacted by the off-road tire, the rim sinkages will gradually converge, and the simulation value is about 53.6 mm in the stable stage.

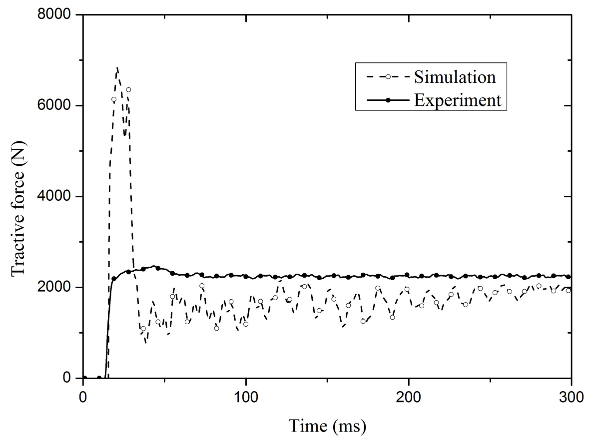

Fig. 9 Simulation and experimental results in terms of the tractive force history

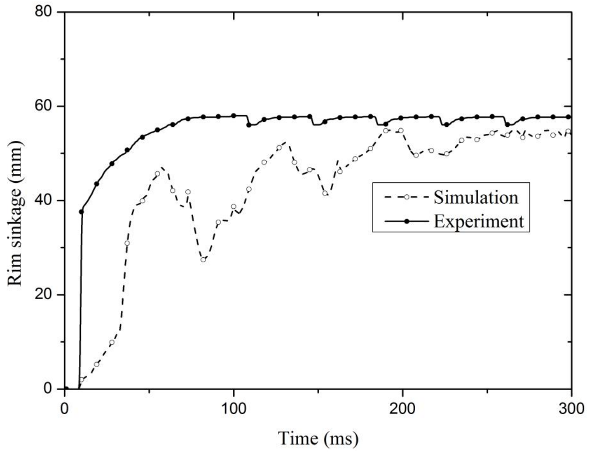

Fig. 10 Simulation and experimental results in terms of the rim sinkage history

6. CONCLUSIONS

In this work, a multi-sphere DE-FE method is developed to investigate the interactions between an off-road tire with smooth tread and gravel terrain. The conclusions are summarized as follows: a) Several kinds of multi-sphere gravel particle models and the combined multi-sphere DE-FE model are established according to the conditions of an indoor soil-bin experiment; b) The developed method is used to analyze the tractive performance of an off-road tire under the slip rate of 20%. The results show that the simulation result of the traveling track of an off-road tire on gravel terrain is consistent with that of experimental result, and the evaluation indexes of the tractive performances obtained by the numerical simulation, including vertical reaction force, tractive force and rim sinkage, are also in agreement with the experimental data. Therefore, our developed method can well predict the traveling behaviors of a tire on granular terrain.

ACKNOWLEDGMENT

This work was supported by a JSPS Grant-in-Aid for Scientific Research (B) (GrantNumber22H03601) and JST FOREST Program (Grant Number JPMJFR215S).

REFERENCES

[1] Nakashima H, Fujii H, Oida A, et al. Discrete element method analysis of single wheel performance for a small lunar rover on sloped terrain. Journal of Terramechanics 2010, 47(5): 307–321.
[2] Nankali N, Namjoo M, Maleki MR. Stress analysis of tractor tire interacting with soil using 2D finite element method. International Journal of Advanced Design and Manufacturing Technology 2012, 5(3): 107–111.
[3] Yang P, Zang M, Zeng H. DEM-FEM simulation of tire-sand interaction based on improved contact model. Computational Particle Mechanics 2020, 7: 629–643.
[4] Nishiyama K, Nakashima H, Yoshida T, et al. FE-DEM with interchangeable modeling for off-road tire traction analysis. Journal of Terramechanics 2018, 78: 15–25.
[5] Zeng H, Xu W, Zang M, et al. Calibration and validation of DEM-FEM model parameters using upscaled particles based on physical experiments and simulations. Advanced Powder Technology 2020, 31: 3947–3959.
[6] Favier JF, Abbaspour-Fard MH, Kremmer M, et al. Shape representation of axisymmetrical, non-spherical particles in discrete element simulation using multi-element model particles, Engineering Computations 1999, 16(4): 467–480.
[7] Wang SP, Nakamachi E. The inside-outside contact search algorithm for finite element analysis. International Journal for Numerical Methods in Engineering 1997, 40(19): 3665–3685.
[8] Balevičius R., Džiugys A, Kačianauska R.. Discrete element method and its application to the analysis of penetration into granular media, Journal of Civil Engineering and Management 2004, 10(1): 3–14.
[9] Guo X, Zheng Z, Zang M, et al. A multi-sphere DE-FE method for traveling analysis of an off-road pneumatic tire on irregular gravel terrain. Engineering Analysis with Boundary Elements 2022, 139: 293–312.